Topology optimization method of metamaterials designfor efficient enhanced transmission througharbitrary-shaped sub-wavelength aperture

Pengfei Shi(史鹏飞), Yangyang Cao(曹阳阳), Hongge Zhao(赵宏革), Renjing Gao(高仁璟), and Shutian Liu(刘书田)

Citation: Chin. Phys. B, 2021, 30 (**9**): 097806. DOI: 10.1088/1674-1056/ac0cde
Journal homepage: http://cpb.iphy.ac.cn; http://iopscience.iop.org/cpb

What follows is a list of articles you may be interested in

Analysis of elliptical thermal cloak based on entropy generation and entransy dissipation approach

Meng Wang(王梦), Shiyao Huang(黄诗瑶), Run Hu(胡润), Xiaobing Luo(罗小兵)
Chin. Phys. B, 2019, 28 (**8**): 087804. DOI: 10.1088/1674-1056/28/8/087804

Broadband microwave absorption properties of polyurethane foam absorber optimized by sandwiched cross-shaped metamaterial

Long-Hui He(贺龙辉), Lian-Wen Deng(邓联文), Heng Luo(罗衡), Jun He(贺君), Yu-Han Li(李宇涵), Yun-Chao Xu(徐运超), Sheng-Xiang Huang(黄生祥)
Chin. Phys. B, 2018, 27 (**12**): 127801. DOI: 10.1088/1674-1056/27/12/127801

Metamaterials and metasurfaces for designing metadevices: Perfect absorbers and microstrip patch antennas

Yahong Liu(刘亚红), Xiaopeng Zhao(赵晓鹏)
Chin. Phys. B, 2018, 27 (**11**): 117805. DOI: 10.1088/1674-1056/27/11/117805

High-performance lens antenna using high refractive index metamaterials

Lai-Jun Wang(王来军), Qiao-Hong Chen(陈巧红), Fa-Long Yu(余发龙), Xi Gao(高喜)
Chin. Phys. B, 2018, 27 (**8**): 087802. DOI: 10.1088/1674-1056/27/8/087802

Controlling flexural waves in thin plates by using transformation acoustic metamaterials

Xing Chen(陈幸), Li Cai(蔡力), Ji-Hong Wen(温激鸿)
Chin. Phys. B, 2018, 27 (**5**): 057803. DOI: 10.1088/1674-1056/27/5/057803

Topology optimization method of metamaterials design for efficient enhanced transmission through arbitrary-shaped sub-wavelength aperture*

Pengfei Shi(史鹏飞)[1,†], Yangyang Cao(曹阳阳)[1], Hongge Zhao(赵宏革)[1], Renjing Gao(高仁璟)[2,‡], and Shutian Liu(刘书田)[2]

[1] College of Marine Electrical Engineering, Dalian Maritime University, Dalian 116023, China

[2] Key Laboratory of Structural Analysis for Industrial Equipment, Dalian University of Technology, Dalian 116023, China

(Received 17 March 2021; revised manuscript received 27 May 2021; accepted manuscript online 21 June 2021)

The electromagnetic wave enhanced transmission (ET) through the sub-wavelength aperture was an unconventional physical phenomenon with great application potential. It was important to find a general design method which can realize efficient ET for arbitrary-shaped apertures. For achieving ET with maximum efficiency at specific frequency through arbitrary-shaped subwavelength aperture, a topology optimization method for designing metamaterials (MTM) microstructure was proposed in this study. The MTM was employed and inserted vertically in the aperture. The description function for the arbitrary shape of the aperture was established. The optimization model was founded to search the optimal MTM microstructure for maximum enhanced power transmission through the aperture at the demanded frequency. Several MTM microstructures for ET through the apertures with different shapes at the demanded frequency were designed as examples. The simulation and experimental results validate the feasibility of the method. The regularity of the optimal ET microstructures and their advantages over the existing configurations were discussed.

Keywords: metamaterial, enhanced transmission, topology optimization, arbitrary-shaped aperture

PACS: 78.67.Pt, 42.25.Bs **DOI:** 10.1088/1674-1056/ac0cde

1. Introduction

Electromagnetic (EM) metamaterial (MTM) is a kind of patterned artificial material with some special EM characteristics, such as negative refraction, band gap, and anti or zero Doppler effect, which the natural materials do not possess.[1–3] The special EM characteristics of MTM can be engendered by the resonance of single MTM microstructure, the coupling between each MTM unit cell, or reasonable MTM unit cell array arrangement. The researchers in the corresponding areas showed great interest in EM MTM in recent years. MTM has been widely used in EM invisibility, sensors, antennas, wave absorbers, and so on.[4–10] It was also found that a reasonable MTM unit cell or coupled MTM pair can be used to achieve enhanced transmission (ET) of EM wave through a sub-wavelength aperture on a metal plate.[11–15]

According to Bethe's theory, the proportion of EM wave transmitting through a sub-wavelength hole on a metal plate was limit, when the radius of the hole was much smaller than the interested wave length.[16] However, Ebbesen's research broke through this restriction. It was found that the light could transmit through the designed aperture array on the silver film.[17] Enlightened by this report, researchers exposed that wave could also transmit through a single aperture on the metallic plate if the resonator with proper form was placed in or near the aperture.[17,18] So far, MTM-based ET has developed into a physical phenomenon across different frequency bands.[19–21] It is of great significance to sensor, aperture imaging and other corresponding fields.[23] MTM resonators based on different resonant mode or coupling mechanisms for the efficient ET through the apertures with different shape and parameters were also proposed successively.[24–28] Zhou inserted the mirror symmetric split ring resonators orthogonally in the circular aperture to enhance the localized field, and achieved ET eventually.[26] For rectangular and square apertures respectively, Xiao *et al.* proposed to realize ET by adjusting the proportion of each part of coplanar T-shaped microstructure embedded in the apertures.[27] In the above research, the transmission characteristics were dependent on the existing microstructures so that it was suitable for a limited aperture shape. By making use of the strong local magnetic resonance, Ramaccia used the connected split ring resonators or omega-shaped resonators to realize ET, which enhanced the transmission with a large enhancement factor and minimize the dependence on the aperture size.[28] If the resonator is too close to the aperture, there would be a strong coupling between the resonator and the aperture. It is uncertain whether a sin-

*Project supported by the National Natural Science Foundation of China (Grant No. U1808215), the Natural Science Foundation of Liaoning Province, China (Grant No. 20180540082), and the Science and Technology Program of Shenzhen (Grant No. JSGG 20200102155001779).

†Corresponding author. E-mail: pfshi@dlmu.edu.cn

‡Corresponding author. E-mail: renjing@dlut.edu.cn

gle configuration is suitable for all aperture shapes. It is still necessary to find the exact corresponding microstructures for different aperture shapes.

Previous studies have shown that the MTM is an effective implementation of ET, but its form is related to the aperture shape.[29,30] There is the demand for the description model of the apertures with different shape. Furthermore, it is necessary to discuss how to find a suitable MTM configuration under the existing aperture description. In the recent years, more and more unpredictable materials or structures with optimal characteristics were designed through topology optimization, which contained the EM MTM microstructures.[31–34] Topology optimization has been proved to be a feasible method for MTM microstructures design under different designing backgrounds. It can also help to get the MTM with proper form for ET with high efficiency through different apertures. Establishing the optimization model of MTM in the ET with high transmission efficiency is also the key problem.

In this study, topology optimization method of MTM design for efficient ET through arbitrary-shaped sub-wavelength aperture at specific frequency was proposed. The optimization model for optimal MTM microstructure design and the model for describing the aperture with different shapes were established. Several numerical examples with different aperture shapes and frequency demands were designed. The simulation and experimental results verified the feasibility of the method. The characteristics of the optimal ET microstructures and their advantages over the existing configurations were discussed. This design method can also be extended to the ET design in other frequency bands.

2. Mechanism analysis and optimization model of MTM

The incident wave can propagate through the waveguide system, but would be cut off if a metallic plate is blocked in the middle. An aperture whose size was much smaller than the working wavelength can not effectively guide the wave to pass. A pair of EM MTM unit cell composed of dielectric substrate and copper microstructures, was orthogonally inserted in the aperture to guide the wave. It was mirror symmetric about the metallic plate, as shown in Fig. 1.[24] Under the excitation of the incident wave, the microstructure at the incident side engendered resonance at the corresponding frequency. The strong electric field near the aperture can be coupled to the neighbor microstructure and transmit the wave into next half waveguide. The part of the microstructure near the aperture can be regarded as an equivalent coupling capacitor or inductor, which helped the wave with same guiding mode passing through the whole waveguide.

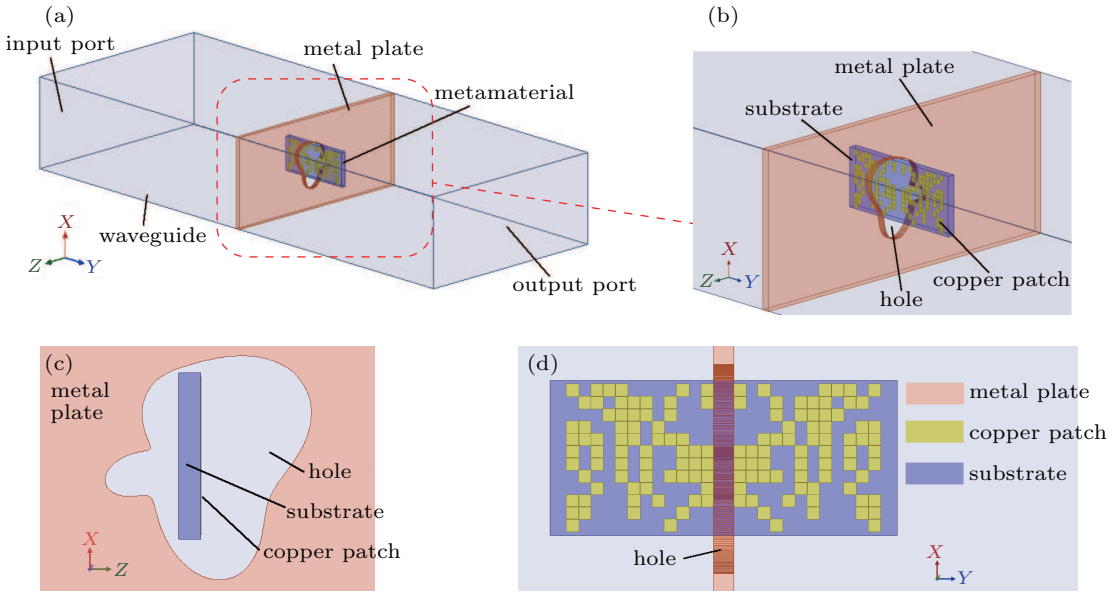

Fig. 1. The aperture and the metamaterial in the waveguide. (a) The waveguide system. (b) The arrangement of MTM in the waveguide. (c) The shape of the hole and the position of MTM. (d) The front view of MTM.

The resonant characteristics, which contained the resonant frequency and the resonant strength, were determined by the configuration of MTM and the coupling between the microstructures and the aperture. In the model establishing, in order to define the arbitrary shape of the hole, the function of the hole $R(\theta;\boldsymbol{r})$ was defined in a two dimensional polar coordinate. The expression of $R(\theta;\boldsymbol{r})$ was

$$R(\theta;\boldsymbol{r}) = r_0 + \sum_{i=1}^{m} r_i \cos(i\theta) + \sum_{j=1}^{n} r_j \sin(j\theta), \tag{1}$$

where angle θ was the polar angle in the polar coordinate. $\boldsymbol{r}$ was the settled weight factor to control the shape of the hole.

After modeling the waveguide and setting the material

and size of MTM, we intended to design the proper microstructure of MTM to obtain maximum transmission at the required frequency. Two copper rectangle regions on the front side of the substrate were denoted as the design domain. Copper patch can be filled or etched in each sub mesh of the periodically discretized design domain. Vector $\boldsymbol{S} = (s_1, s_2, s_3, \ldots, s_n)^{\mathrm{T}}$ was used as design variable. Each element s_i in $\boldsymbol{S}$ was binary for presenting the absence or presence of the copper patch in each sub mesh.

The design domain was mirror symmetric, so only half of the vector $\boldsymbol{S}$ was coded and the other half was the same as the coded part. This kind of coding ensured the arranging of the patches in the whole design domain, and decreased twice coding quantity simultaneously. It was helpful for improving the optimization efficiency. Meanwhile, in order to avoid the situation that too much computing resources were invested in the infeasible solution of complex microstructure, the rough finite element grid was used to calculate the numerical value of the model at first. If there was ET characteristics, the grid was refined to calculate the exact solution. Too much calculation on the unnecessary microstructure was avoided in order to improve the optimization efficiency.

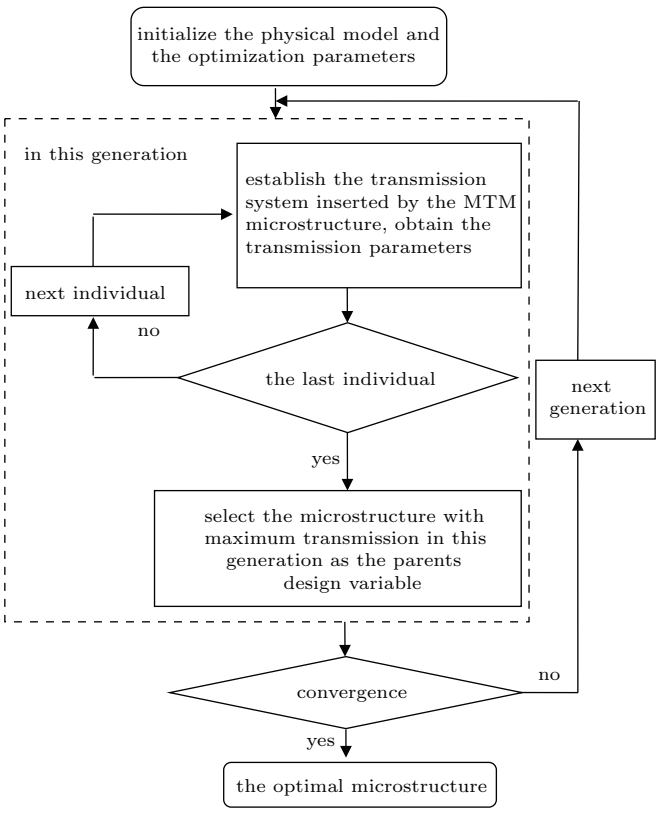

Fig. 2. Flow chart of the optimization design.

The transmission efficiency of the model can be represented by S_{21} parameters of the two port networks, which can be obtained by solving the transmission system (in this study, FEM-based software HFSS was employed). Genetic algorithm was chosen as the optimization algorithm. Matlab was used to control the iteration and the convergence of the optimization process. For high efficiency of ET at the demanded frequency, the design object was to find the optimal design variable $\boldsymbol{S}$, to get the maximum S_{21} at the specific frequency f_{r}. The optimization function was as below:

$$\begin{aligned} &\text{find} \quad \boldsymbol{S} = (s_1, s_2, s_3, \ldots, s_n)^{\mathrm{T}}, \\ &\max_{\boldsymbol{S}} \quad F(\boldsymbol{S}; f_{\mathrm{r}}) = S_{21}. \end{aligned} \tag{2}$$

The flow chart of the optimization design was shown in Fig. 2.

3. MTM design for ET at specific frequency

Numerical examples were designed to validate the robustness of the method. In the first two examples, the interested frequency range was 8 GHz to 12 GHz. The cross section of waveguide was 22.86 mm × 10.16 mm. The 0.5-mm thick metal plate was placed in the middle of the waveguide. The substrate of MTM was FR4, whose dimension was 8.5 mm × 3.8 mm × 0.5 mm. Half of the design domain was 3.6 mm × 3.6 mm. It was discrete and each sub mesh was 0.3 mm × 0.3 mm. The patch in the sub mesh was 0.31 mm × 0.31 mm. The distance between the two sub design domain d was 0.5 mm.

In the first example, the hole was a 2-mm radius circle and positioned at the center of the plate, as shown in Fig. 3(a). The shape of the hole was defined by function (1), in which the weight factor $r_0 = 2$ mm, and other elements in vector $\boldsymbol{r}$ were zero. The maximum transmission at 11.5 GHz was required. In different numerical examples, by using personal computer with Intel Core i7-8700k 3.70-GHz CPU and 16-GHz memory, the optimization running time was about 48 hours to 168 hours. In this example, the optimization running time was 94 hours. The transmission efficiency through the aperture without the MTM was less than −30 dB, which meant the wave could not pass the aperture in this situation. The topology optimized configuration was shown in Figs. 3(a) and 3(b). The maximum transmission at 11.5 GHz was −1.35 dB. Figure 3(e) illustrated that there was a peak of S_{21} of the optimized microstructure at 11.5 GHz. The power loss was also calculated according to the simulated reflection and transmission coefficients as $L = 1 - |S_{21}|^2 - |S_{11}|^2$. There was about 20% power loss near the ET frequency, which was mainly from the dielectric loss of the substrate in resonance. Because at the microwave band the copper was approximated as perfect electrical conductor, the conductor loss was limited. Selecting a kind of substrate with low loss tangent can effectively decrease the loss in resonance.

The designed MTM microstructure was validated experimentally. The MTM microstructure was manufactured by etching technique. The rectangle straight waveguide was connected with vector network analyzer (VNA). The tested specimen and experimental platform was shown in Figs. 3(c) and 3(d). The tested S parameters of the waveguide system with

the designed MTM microstructure were shown in Fig. 3(f). The tested S parameters coincided with the simulated results. The transmission efficiency at 11.5 GHz was −1.87 dB. The maximum transmission was −1.84 dB at 11.505 GHz. Without MTM, the S_{21} parameter was below −30 dB, so the transmission was blocked in the whole frequency band.

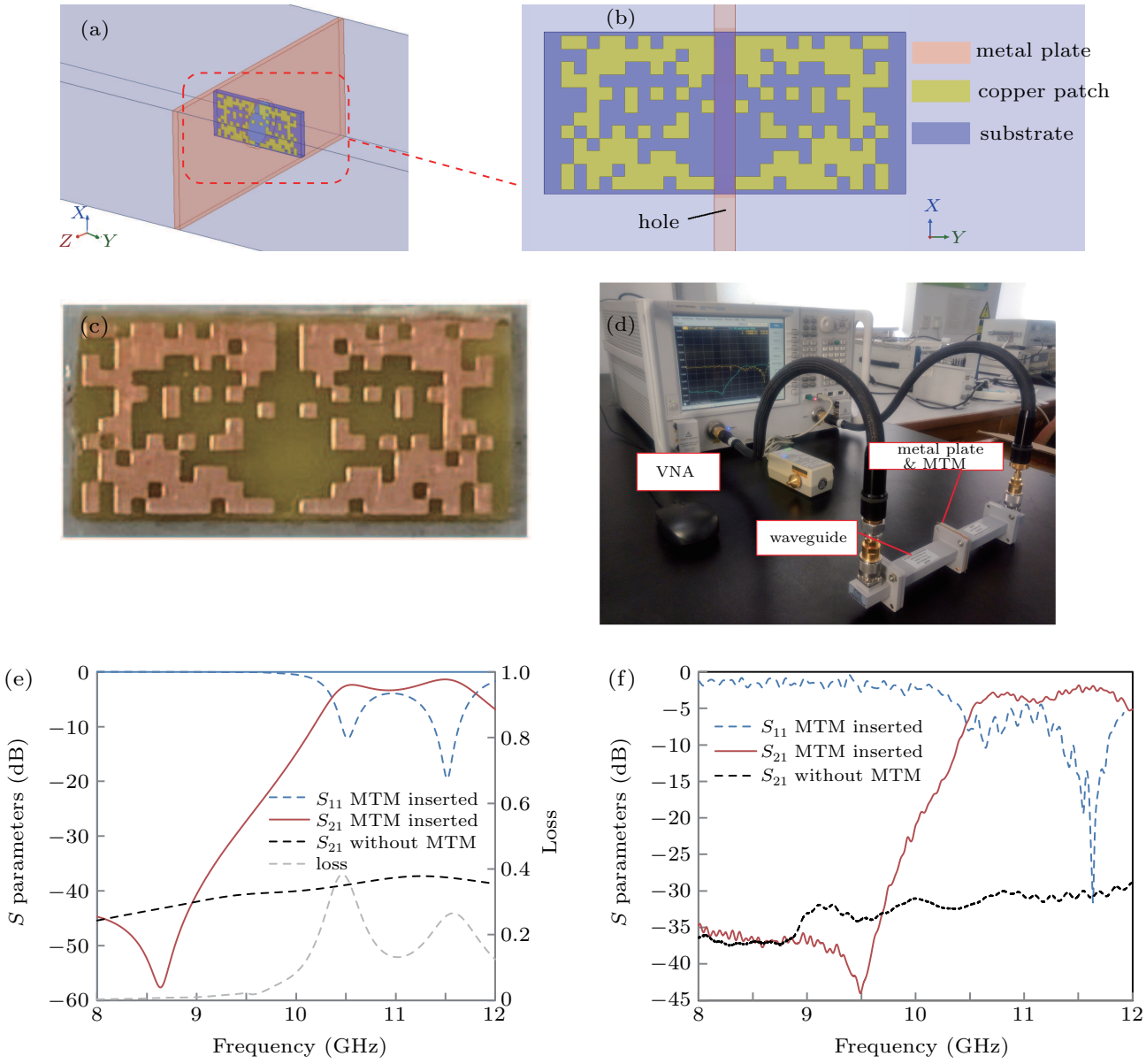

Fig. 3. The designed MTM and its transmission characteristics. (a) The arrangement of MTM in the aperture. (b) The front view of the designed MTM. (c) The specimen of MTM and (d) the experimental platform. The transmission characteristics (e) from simulation and (f) from experiment. The red solid line, the blue dashed line and the grey dashed line were the S_{21}, S_{11}, and the loss of the transmission system inserted with the designed MTM microstructure. The black dotted line was the S_{21} of the transmission system without MTM.

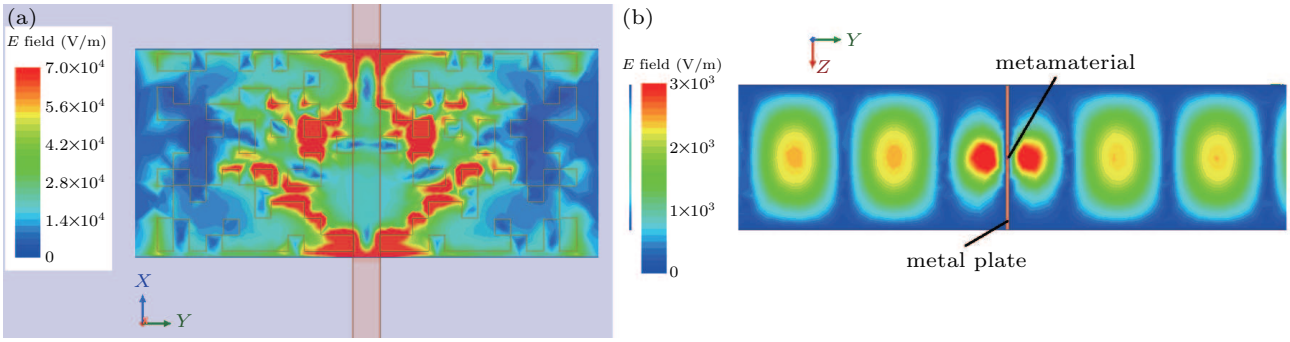

Fig. 4. The electric field distribution at 11.5 GHz. (a) The electric field distribution on the MTM. (b) The electric field distribution in the waveguide with the designed MTM microstructure in the aperture.

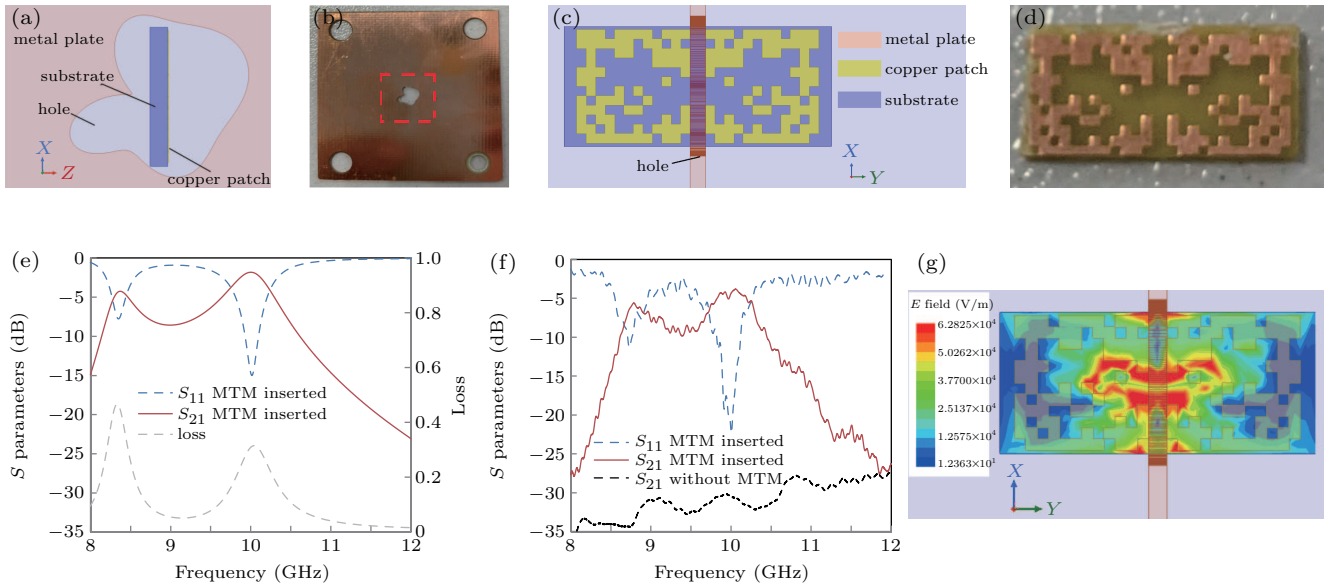

Fig. 5. The aperture, the designed MTM and the transmission characteristics. (a) The perspective and (b) the specimen of the aperture. (c) The front view and (d) the specimen of the designed MTM microstructure. The transmission characteristics (e) from simulation and (f) from experiment. (g) The electric field distribution on MTM.

A further study on the coupling between the two parts of the MTM was carried out. Under the TE10 mode wave excitation, time varying magnetic field excited local resonance in the MTM. A strong electric field was generated under the resonance near the aperture, as shown in Fig. 4(a). An equivalent capacitance effect was created and coupled the two parts. On the analysis of the electric field in the whole waveguide, as shown in Fig. 4(b), there was a strong local field on both sides of the metal plate engendered by MTM, which guided the wave passing through the aperture.

In the second example, an irregular shape was chosen as the shape of the aperture. The maximum transmission at 10 GHz was required. The indicator $\boldsymbol{r}$ in the function (1) was $[r_0; r_i; r_j] = [0.002014; 0.00076; 0, 0.00038, -0.000304, 0.00038]$, and the corresponding irregular shape of the hole was established by the expression as

$$R(\theta; \boldsymbol{r}) = 0.00038 \times \big[5.3 + 2\cos(\theta) + \sin(\theta) - 0.8\sin(3\theta) + \sin(4\theta)\big]. \quad (3)$$

The shape of the aperture was shown in Figs. 5(a) and 5(b). The other parts in the transmission system were the same as the ones in the first example. The designed MTM microstructure and its specimen were shown in Figs. 5(c) and 5(d). The transmission at 10 GHz was −1.826 dB in the simulation. From the experiment, the maximum S_{21} was −3.8 dB at 10.06 GHz, and was −4.3 dB at 10 GHz. The electric field distribution indicated that there was a strong electric coupling on the gap of the microstructure near the aperture, where the electric field was concentrated. The strong local coupling guided the efficient transmission.

4. Discussion

4.1. Configuration analysis

Through the calculation of a certain number of examples, it was found that under different design constraints, the optimized microstructures showed a kind of regularity. The region without metal or without continuous metal patches mainly concentrated in the cental area, while the region outside was surrounded by the continuous metal patches, as shown in Figs. 3(b) and 5(c) in the numerical example 1 and numerical example 2. The surrounding continuous metal patches in the microstructures were easy to exhibit a strong resonance in a defined design domain. According to the equivalent circuit theory, the two cavities formed by the surrounding continuous metal patches on both sides of the MTM produced corresponding equivalent parallel double tuned *LC* circuits. In different microstructure forms, the circuits on both sides realized capacitive coupling with capacitor C_c or inductive coupling with mutual inductance M, as shown in Figs. 6(a) and 6(b). The *LC* circuit realized the coupling between the primary and secondary circuits under its own resonant state. On this basis, the adjustment of patch composition in the design domain was the adjustment of the equivalent *LC* resonant circuit and the coupling form.

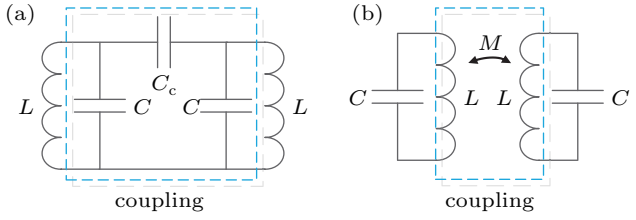

Fig. 6. The equivalent double tuned LC circuits of MTM. (a) The capacitive coupling. (b) The inductive coupling.

4.2. Comparison with the typical microstructure

The results of the above examples verified the feasibility and robustness of the proposed method for obtaining the optimal ET MTM. The proposed design method was helpful for finding a corresponding feasible solution for different design constraints and requirements. In order to highlight the generality and advantages of the proposed method, the results of topology optimization were compared with the ET performance of the waveguide system inserted with the typical MTM microstructure. A typical MTM microstructure, single split ring (SSR), was selected as a comparison. According to the aperture and required frequency of the example 1 and example 2, the optimal SSR was obtained in the same preparation precision. The corresponding ET characteristics were simulated, as shown in Figs. 7(a) and 7(b). At the required frequency 11.5 GHz and 10 GHz, the corresponding S_{21} was -1.48 dB and -2.19 dB respectively. The S_{21} of the waveguide system inserted with the topology optimized MTM at the specific frequency was slightly higher than that of the SSR-inserted one. In the above two examples, despite the constraints of aperture and design domain, the specified design domain and location were sufficient to provide enough electric length space and coupling coefficient for MTM resonance at the required frequency, so the feasible solution of SSR can be obtained.

Under small irregular apertures, design domains and weak coupling constraints, the existing microstructures may not have feasible solutions, and the proposed method can be employed to solve this kind of problems. A comparative example was carried out. The aperture and design domain was adjusted. The expression of the aperture was

$$R(\theta;\boldsymbol{r}) = 0.00032\times\left[5.3+2\cos(\theta)+\sin(3\theta) -\sin(4\theta)+\cos(5\theta)\right]. \quad (4)$$

The required specific ET frequency was 9 GHz, and the size of the inserted MTM substrate was 7.7 mm × 3.2 mm × 0.5 mm. The scope of microstructure design domain was 3 mm × 3 mm, which was discreted into 10 × 10 grid array. The distance between the two sub design domain d was 1.5 mm. The aperture shape and the designed MTM microstructure were shown in Figs. 8(a) and 8(b). The S parameters of the waveguide system were shown in Fig. 8(c). At 9 GHz, the S_{21} of the waveguide system inserted with the topology optimized MTM was -5.16 dB. However, due to the limitation of the design domain and the weak coupling between the two SSR, resonance could not be generated under the 9 GHz excitation. No reasonable feasible solution of SSR can be found. The maximum S_{21} at 9 GHz of the optimal SSR was -28.12 dB. The proposed method can improve the ET efficiency of the existing typical microstructure, and can help to solve the problem that the existing microstructures may have no feasible solution under some specific constraints. It can avoid the dependence on the aperture and the design domain, and showed stable performance in feasible microstructures design.

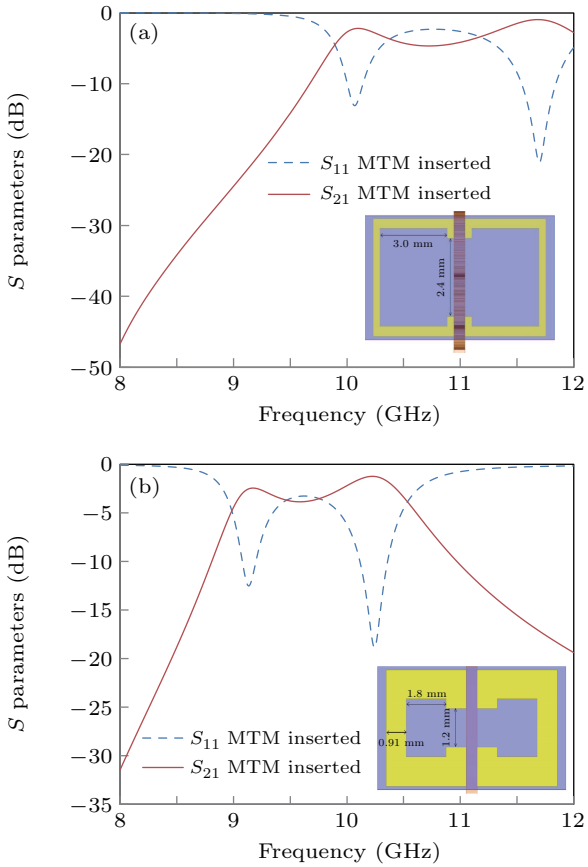

Fig. 7. The S parameters of the waveguide system with SSR. The S parameters of the waveguide system inserted with the optimal SSR with the maximum S_{21} (a) at 11.5 GHz and (b) at 10 GHz.

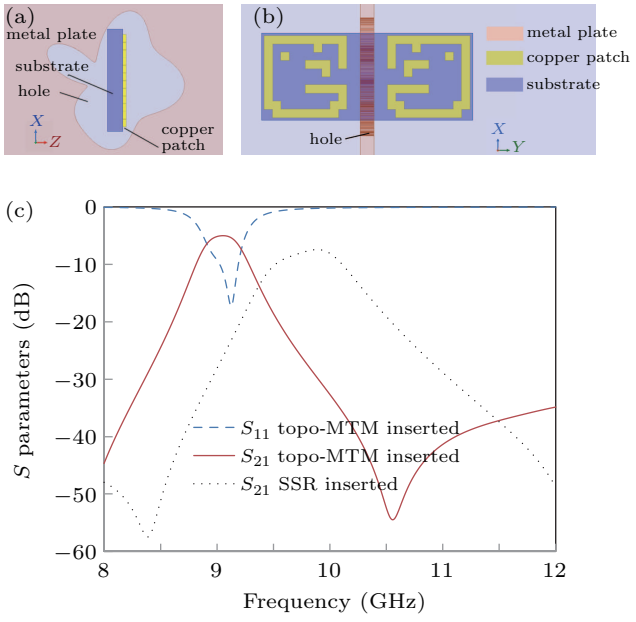

Fig. 8. The aperture, the designed MTM and the S parameters. (a) The perspective of the aperture. (b) The front view of the designed MTM microstructure. (c) The S parameters of the waveguide system from simulation.

5. Conclusion

The topology optimization method for designing MTM microstructure in the ET through the aperture with arbitrary shape was proposed. The arbitrary shape of the aperture was described by the sum of a series in sine or cosine form. The copper patch arrangement in the discrete design domain was chosen as the design variable, and the highest power transmission through the aperture at a specific frequency was chosen as the designing target. The numerical examples for different transmission frequency demands were conducted respectively. The electric field distribution illustrated that there was a strong coupling on the microstructures near the metal plate at the demanded frequency, so that the designed microstructure can engender efficient transmission enhancement. The experimental results were consistent with the simulated ones, which also validated the feasibility of the method. The regularity of the optimal ET microstructures and the characteristic comparison with the typical MTM microstructure were analyzed.

References

[1] Wiltshire M C, Pendry J B, Young I R, Larkman D J, Gilderdale D and Hajnal J V 2001 *Science* **291** 849
[2] Shelby R A, Smith D R and Schultz S 2001 *Science* **292** 77
[3] Ran J, Zhang Y, Chen X D, Fang K, Zhao J and Chen H 2016 *Sci. Rep.* **6** 23973
[4] Jiang Q, Xiang C, Luo Y, Wu L, Zhang Q, Zhao S, Qin F and Lin J 2020 *Mater. Design* **185** 108270
[5] Yi J, Campbell S D, Feng R, Burokur S N and Werner D H 2018 *Opt. Express* **26** 505
[6] Zhu J, Lao C, Chen T and Li J 2020 *Mater. Design* **191** 108618
[7] Kandwal A, Li J, Igbe T, Liu Y, Li S, Wang L, Hao Y and Nie Z 2020 *Sci. Rep.* **10** 113
[8] Liu T and Kim S 2019 *Sci. Rep.* **9** 16494
[9] Mei Y H, Shao Y and Hang Z H 2019 *Acta Phys. Sin.* **68** 227803 (in Chinese)
[10] Yang X, Wei T, Chen F, Gao F, Du J and Hou Y 2020 *Chin. Phys. B* **29** 107303
[11] Wen J, Wang K, Feng H, Chen J, Gao X, Hong R and Zhang D 2017 *Plasmonics* **12** 1257
[12] Lee I, Sohn I, Kang C, Kee C, Yang J and Lee J W 2017 *Opt. Express* **25** 6365
[13] Cetin A E, Turkmen M, Aksu S, Etezadi D and Altug H 2015 *Appl. Phys. B* **118** 29
[14] Hu Y, Liu G, Liu Z, Liu X, Zhang X, Cai Z, Liu M, Gao H and Gu G 2015 *Plasmonics* **10** 483
[15] Fan J, He Y, Jiao Y, Hao L, Zhao J and Jia S 2021 *Chin. Phys. B* **30** 034207
[16] Bethe H A 1944 *Phys. Rev.* **66** 163
[17] Ebbesen T W, Lezec H J, Ghaemi H F, Thio T and Wolff P A 1998 *Nature* **391** 667
[18] Zhu H, Yao A and Zhong M 2016 *Chin. Phys. B* **25** 107301
[19] He M, Ma W and Wang X 2013 *Chin. Phys. B* **22** 114201
[20] Wang Y, Duan G, Zhang L, Ma L, Zhao X and Zhang X 2018 *Sci. Rep.* **8** 2087
[21] Liang T, Shao W, Wei X and Liang M 2018 *Chin. Phys. B* **27** 100204
[22] Kang E S H, Ekinge H and Jonsson M P 2019 *Opt. Mater. Express* **9** 1404
[23] Yuan J, Kan Q, Geng Z, Xie Y, Wang C and Chen H 2014 *Chin. Phys. B* **23** 084201
[24] Malyuskin O and Fusco V 2017 *Sens Imaging* **18** 7
[25] Guo Y S, Zhou J, Lan C W, Wu H Y and Bi K 2014 *Appl. Phys. Lett.* **104** 204103
[26] Hajian H, Ozbay E and Caglayan H 2017 *Sci. Rep.* **7** 4741
[27] Guo Y and Zhou J 2015 *Sci. Rep.* **5** 8144
[28] Xiao S, Peng L and Mortensen N A 2010 *Opt. Express* **18** 6040
[29] Ramaccia D, Palma L D, Ates D, Ozbay E, Toscano A and Bilotti F 2014 *IEEE Trans. Antennas Propag.* **62** 2093
[30] Azemi S N and Rowe W S 2018 *IEEE Antennas Wireless Propag. Lett.* **17** 2246
[31] Wang Y, Qin Y and Zhang Z 2014 *Plasmonics* **9** 203
[32] Lim H, Yoo J and Choi J S 2014 *Struct. Multidisc. Optim.* **49** 209
[33] Jung J, Goo S and Kook J 2020 *Mater. Design* **191** 108627
[34] Diaz A R and Sigmund O A 2010 *Struct. Multidisc. Optim.* **41** 163
[35] Lin Z, Liu V, Pestourie R and Johnson S G 2019 *Opt. Express* **27** 15765